SAE INTERNATIONAL

ARTICLE INFO
Article ID: 14-15-02-0007

doi:10.4271/14-15-02-0007

Economic Feasibility Analysis of Second-Life Batteries in Electric Bus Charging Station at Stanford

Jihan Zhuang,[1] William Chueh,[1] Simona Onori,[1] and Sally M. Benson[1]

[1]*Stanford University, USA*

Abstract

Currently, a persistent concern arises regarding the management of retired Li-ion batteries from electric vehicles (EVs). A potential solution is to repurpose these batteries for less demanding applications, such as energy storage systems. Such repurposed batteries are commonly referred to as second-life batteries (SLBs). In this work, we explore the economic feasibility of implementing SLBs in Stanford University's EV bus charging station via previously developed technoeconomic decision support model. The model simulates battery aging behaviors across various usage conditions, optimizing the operational parameters of SLBs. The estimated lifetime is expected to be 10 years in an optimal using condition. In addition, an economic sensitivity analysis explores the influences of various factors. Furthermore, we calculate the cost savings of total $82,500 over its second lifetime, which is derived from the adoption of SLB instead of new batteries.

History

Received: 03 Jun 2025
Revised: 27 Nov 2025
Accepted: 19 Feb 2026
e-Available: 16 Mar 2026

Keywords

Second-life battery, Decision support model, Stanford EV bus charging station

Citation

Zhuang, J., Chueh, W., Onori, S., and Benson, S., "Economic Feasibility Analysis of Second-Life Batteries in Electric Bus Charging Station at Stanford," *SAE Int. J. Elect. Veh.* 15(2):2026, doi:10.4271/14-15-02-0007.

ISSN: 2691-3747
e-ISSN: 2691-3755

1. Introduction

In March 2022, Stanford University successfully transitioned to 100% renewable electricity, surpassing the annual energy consumption of its on- and off-campus facilities through renewable electricity generation [1]. In particular, the university has been actively electrifying its diesel bus system since 2014, resulting in a fleet of electric buses operating on campus by 2020 [2]. These electric buses are using LFP (Lithium Iron Phosphate) battery chemistry and supported by charging stations that rely on solar power generated on campus. However, due to the operation time of the solar Photovoltaic (PV) systems (only during daytime), the charging stations still draw some carbon-based electricity from the grid. As a result, the charging process remains partially carbon-emitting. To address this issue and achieve decarbonized bus charging, a project has been initiated to demonstrate a 24/7 carbon-free electrified campus bus fleet. The project aims to develop a scalable platform that intelligently coordinates solar energy, energy storage, electric bus route assignments, and bus charging. The platform objectives include minimizing energy costs, ensuring system resiliency, and optimizing vehicle utilization throughout the campus [3].

Numerous studies in the literature have focused on examining the economic viability of utilizing SLBs in combination with PV systems at EV charging stations [4, 5]. In 2013, Tong et al. [6] conducted a feasibility study on the implementation of an SLB pack in an off-grid PV vehicle charging system. The battery pack consisted of 135 LFP SLBs and was projected to have a lifespan of 5.5 years in that particular application. They set up a demonstration system in the Sacramento, CA area and evaluated its performance through numerical simulations and experimental testing. The study's findings, based on both experimentation and simulation, demonstrated the feasibility and cost-effectiveness of incorporating SLBs in charging stations integrated with PV systems, as compared to systems utilizing new Li-ion batteries. Similarly, Hamidi et al. [7] investigated the integration of wind power, solar PV power, and Li-ion battery energy storage into a DC microgrid-based charging station for EVs. They proposed the integration of SLBs into the system to serve as an energy buffer and provide emergency power in the event of a grid connection loss.

In a recent study [8], researchers examined the real-world performance of an SLB in three different scenarios, including a fast-charging station for electric buses. Experimental analysis revealed that the SLB experienced greater degradation in the fast-charging station for urban buses compared to energy storage for a residential PV system, attributed to the demanding operating conditions (higher C-rate) compared to the other scenarios. The researchers also concluded that oversizing the SLB would be necessary to ensure economic profitability. Another study [9] conducted a case study involving an integrated system consisting of an SLB, a PV generator, and a grid-connected mobile network telecommunication station. Similarly, SLBs were employed for energy peak power shaving and shifting purposes. The model results demonstrated significant potential for cost reduction, both in economic and environmental terms, through the utilization of SLBs. Kamath et al. [10] investigated the economic costs and life cycle environmental impacts of implementing SLBs in five cities across the United States. Compared to the use of new batteries, the adoption of ORCID(s): SLBs resulted in a reduction in the levelized cost of electricity (LCOE) by 12–41% and the global warming potential (GWP) by 7–77%. Furthermore, when combined with PV systems, SLBs further decreased reliance on grid electricity, leading to greater reductions in GWP and cumulative energy demand (CED) compared to using SLBs alone.

It is worth noting that the economic analysis conducted on SLBs mentioned earlier primarily relies on cell-level degradation models, overlooking the uncertainties associated with battery module/pack-level aging. Disassembling SLBs into individual cells is costly [11], necessitating the development of effective simulation tools for battery aging models at the module level. Factors such as electrical configuration, cell inhomogeneity, and cell-to-cell thermal interactions can result in varying degrees of degradation among cells within battery modules, introducing uncertainties in overall degradation. Seger et al. [12] explored the influence of individual cell uncertainties on module capacity and emphasized the importance of considering these effects when developing aging models at the module level. Therefore, in this article, we employ the technoeconomic decision support model developed in the previous paper [13], which contains a module-level battery degradation model and economic model, to simulate SLB module degradation and its economic feasibility specifically within an EV bus charging station at Stanford. This article focuses on developing an LFP-specific battery aging model, conducting a detailed sensitivity analysis of the economic framework, and evaluating the feasibility of SLB deployment in a real-world application. In contrast, our previous work centered primarily on the overall framework design and conceptual demonstration.

1.1. LFP Battery Aging Models

Considering the disparity between the battery chemistries employed in the EV buses at Stanford and the cells utilized in [13], the developed prediction model designed for NCA Tesla cells in such a model framework is incompatible in this scenario. To address this challenge, a viable solution involves substituting the original cell-level aging model with a new model specifically designed for LFP batteries.

In the literature, there are different types of battery degradation models, including physics-based models

[14–16], empirical/semi-empirical models [17–19], and data-driven models [20, 21]. The empirical/semi-empirical models curve-fit the relationship of various stress factors, such as temperature, C-rate, and Depth of Discharge (DoD), onto the data, resulting in a relatively simple analytical formula. Their simplicity allows using those aging models in a wide variety of studies, such as system-level design problems, optimization models, and battery management systems [22]. In addition, the analytical formulas give a direct indication of the effect of various stress factors.

Battery aging encompasses cycling and calendar aging. Wang et al. [19] introduced a cycle-life model tailored for LFP batteries. Their data collection involved varied parameters: temperature (–30°C to 60°C), DoD (ranging from 90% to 10%), and discharge rate (C-rate from C/2 to 10C, with 1C corresponding to 2A). They formulated two equations for high and low C-rates within their cycle-life model. These equations governed capacity loss, relating it to time or charge throughput through a power law, while temperature effects were accounted for using an Arrhenius correlation. Regarding calendar life aging, Sarasketa-Zabala et al. [23] established a comprehensive model for LFP batteries. Their study included five static calendar aging conditions, involving varied storage temperatures and State of Charge (SOC) levels, to assess cell degradation. Validation encompassed both constant operating conditions and dynamic scenarios. Model predictions closely aligned with experimental results, displaying a root-mean-square error of 0.93% for experiments lasting between 300 and 650 days. In a recent study, Najera et al. [18] analyzed capacity degradation modeling in LFP batteries, considering both calendar and cycling aging. Their developed aging model accounted for variations in key parameters defining the model: temperature, DoD, and charge/discharge rate. The proposed battery aging model demonstrated a maximum relative error of 3%, varying based on specified working conditions.

Based on the above analysis, in this work, we opted to develop a semi-empirical model for LFP cells, using similar mathematical equations from the literature.

1.2. Article Objective and Structure

The primary aim of this study is to evaluate the economic viability of integrating SLBs into the EV bus charging station at Stanford University. Prior research has showcased successful instances of incorporating SLBs into EV charging stations, often coupled with PV systems. Hence, our focus is on conducting a case study involving the Stanford Marguerite Shuttle, a sizable electric bus fleet, utilizing a technoeconomic decision support model outlined in our previous publication [13].

However, since the battery energy storage system (BESS) has not yet been deployed, the analysis is based on projected operational conditions and design assumptions rather than measured field data. In this application, the SLB system stores surplus solar PV energy during daylight hours and discharges at night to supply the EV bus charging station. A typical setup for BESS combined with PV can refer to a real-world project [24], and the cooling system for BESS is normally designed by battery OEMs such as Honeywell [25] and BYD [26]. Here, we assume the BESS would follow the OEMs' default setup.

Rather than directly applying the same model used previously, this study involves developing a semi-empirical model for LFP batteries, intended to replace the data-driven model initially developed for NMC chemistry in the decision support model framework. Subsequently, the cell-level model is incorporated into the same module-level aging model framework. Various aging factors are well examined, and optimal operational conditions are derived based on simulation outcomes. The projected lifespan derived from these models feeds into the identical economic model detailed in our prior work [27], enabling the calculation of SLB value.

Under the assumption that acquiring used batteries from EV buses incurs negligible costs, this approach allows for the calculation of cost savings achievable by implementing SLBs instead of entirely new ones throughout the SLB's operational span. Furthermore, a sensitivity analysis is conducted to explore how different variables could influence cost savings, examining both best-case and worst-case scenarios. This analysis aims to provide a comprehensive understanding of the potential cost benefits associated with this implementation.

The article is organized as follows: Section 2 delineates the methodology employed in this study. Section 3 elaborates on our modeling approach for the semi-empirical aging model of LFP batteries. In Section 4, we present the outcomes stemming from both the cell-level semi-empirical model and the module-level simulations. Additionally, this section includes the computed cost savings derived from our economic model. Lastly, Section 5 encapsulates the conclusions drawn from this work and proposes potential avenues for future research.

2. Methodology

2.1. Experimental Dataset

The dataset utilized in this section to examine battery cycle aging was sourced from Sandia National Lab (SNL) [28]. This dataset encompasses data generated under various temperatures and discharging conditions. The LFP batteries used belong to the A123 system, each possessing a nominal capacity of 1.1 Ah. The electrode

TABLE 1 LFP battery information and cycling conditions.

Battery chemistry	Manufacturer	Nominal capacity	Temperatures	DoDs	Charge protocols	Discharge protocols
LFP	A123	1.1 Ah	15/25/35	20%/60%/100%	0.5C CC-CV	0.5C/1C/2C/3C CC

stacking method of the LFP cylindrical cell used in the experiment is a winding. Here, we assume the SLBs implemented will have the same chemistry, cell form factor, and stacking method.

All battery cells underwent consistent charging protocols, involving a 0.5C Constant Current (CC) Charge succeeded by a Constant Voltage (CV) charge. However, diverse CC discharging profiles were employed, incorporating distinct current rates (0.5C, 1C, 2C, and 3C), varying DoD levels (100%, 60%, and 20%), and different operating temperatures (15°C, 25°C, and 35°C). Detailed battery information and the experimental configuration are presented in Table 1. For more details, additional information is available on the referenced website [29]. In this article, only 100% DoD data are used to develop the model, as the partial DoD datasets (60% and 20%) exhibited negligible degradation (capacity remains nearly unchanged after 3000 cycles) and represented a small portion of the available test conditions (5 out of 30 test cases). It is noted that the absence of partial DoD cycling data may lead the model to underestimate SLB lifetime; however, this results in a conservative prediction that remains valid as an upper-bound estimate under full-depth cycling conditions.

The degradation curves depicting LFP performance under different C-rates and temperatures are illustrated in Figure 1. These curves offer a comprehensive view of the battery's response to varying operational conditions, crucial for understanding the aging dynamics of the cells.

FIGURE 1 LFP battery degradation curves under various experimental cycling conditions.

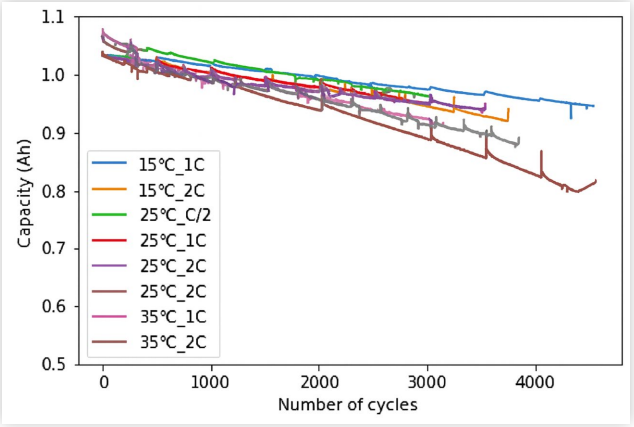

2.2. Semi-empirical Cell-level Model

Li-ion battery cell's degradation consists of calendar aging (denoted as Q_{cal}) and cycling aging (denoted as Q_{cyc}), which is expressed in Equation 1.

$$Q_{cell} = Q_{cal} + Q_{cyc} \tag{1}$$

The calendar aging of batteries illustrates degradation during storage periods when the cell experiences no electrical current flow. Primarily, two key variables impact calendar aging: temperature and SOC. The influence of these parameters on calendar aging varies based on the specific battery chemistry.

Equation 2 adopts an Arrhenius exponential expression, serving to estimate the relationship between these variables and calendar aging. This equation models the capacity fade over time, capturing the dependence on temperature and SOC variables [17, 30].

$$Q_{cal} = g \cdot e^{h \cdot SOC} \cdot e^{I/T} \cdot t^{z} \tag{2}$$

In the above equation, T represents the battery temperature, while t signifies time. The SOC stands for the mean SOC of the charge/discharge process, which equals the average value of the maximum and minimum SOCs. Additionally, three parameters (g, h, and I), contingent upon the battery's chemistry, are employed to tailor the model to each specific battery. The parameter z, known as the power law factor, typically ranges between 0.5 and 1.

Contrarily, aging during cycling of Li-ion batteries is attributed to kinetic-induced effects [31]. This degradation primarily hinges on the battery's operational mode, specifically the selected current profile and operating temperature. Additionally, battery chemistry influences the capacity loss incurred during cycling processes. Although various semi-empirical models exist in the literature to represent cycling aging, the model presented in this work employs and modifies Equation 3, which is commonly found in previous papers [17–19].

$$Q_{cyc} = \left(a \cdot T^2 + b \cdot T + d\right) \cdot e^{\left(f \cdot T + s\right) \cdot \left(p \cdot C_{rate} + q\right)} \cdot AH \tag{3}$$

where AH denotes the capacity through-output in Ah, while C_{rate} represents the charge and discharge current applied to the battery concerning its nominal capacity. Similar to the case of calendar aging, a set of model parameters (a, b, d, f, s, p, and q), contingent upon the

battery's chemistry, is established to customize the model for each specific battery. These parameters facilitate the adaptation of the model to the distinct characteristics of individual batteries.

According to the expressions exposed above, Equation 1 can be rewritten as:

$$Q_{cell} = \left(a \cdot T^2 + b \cdot T + d\right) \cdot e^{\left(f \cdot T + s\right) \cdot \left(p \cdot C_{rate} + q\right)} \cdot AH + g \cdot e^{h \cdot SOC} \cdot e^{l/T} \cdot t^z \quad (4)$$

In Equation 4, Q_{cell} represents the final capacity fade in percentage, T denotes the battery temperature in Kelvin, AH signifies the capacity through-output in Ah, C_{rate} pertains to the discharge rate, t represents time in seconds, and z stands for the power law factor. Additionally, parameters a, b, d, f, g, h, l, s, p, and q are contingent upon the battery chemistry, offering vital dependencies within the equation. For example, the LFP battery shows slower capacity fade under moderate cycling conditions, lower thermal runaway risk, and longer cycle life, making the parameters relatively smaller. In contrast, NMC battery is generally more sensitive to aggressive cycling such as high temperature and high SOC operation range. Although the present model is calibrated for LFP battery as it's more suitable for second-life applications, the modeling framework is chemistry-agnostic and can be extended to other chemistries by adjusting the empirical degradation parameters based on chemistry-specific datasets.

This equation (4) serves to calculate the degradation of LFP cells and can be seamlessly integrated into the module-level degradation model. For an in-depth understanding of the cell-level semi-empirical model and its parameter identification, detailed insights can be found in [18]. The specific model parameters utilized in our case are outlined in Table 2. These parameters play a crucial role in tailoring the model to the distinctive characteristics of the batteries under consideration. While formal confidence intervals were not calculated for the fitted parameters, model validation was performed using R^2 and mean absolute error (MAE) metrics, and stochastic variability was introduced at the module level via Monte Carlo simulations to partially account for uncertainty in parameter values.

TABLE 2 Parameters in the LFP semi-empirical aging model.

Parameters	Values
a	$-8.345 \cdot 10^{-9}$
b	$2.252 \cdot 10^{-7}$
d	$9.738 \cdot 10^{-4}$
f	$2.452 \cdot 10^{-4}$
s	0.2371
p	5.335
q	4.435
g	$5.980 \cdot 10^{6}$
h	−7.245
l	$-6.988 \cdot 10^{3}$
z	0.7672

2.3. Module-level Simulation Model

After the cell-level aging model is developed, it is integrated into the module-level model via simply replacing the Gaussian Process Regression (GPR) model in the module-level model framework as [13] described. The module-level aging simulation is carried out in three sequential steps.

First, the semi-empirical cell-level degradation model predicts each cell's capacity and resistance evolution over time. In the absence of measured resistance data, we assumed an inverse proportionality between capacity retention and internal resistance, consistent with empirical aging trends [32–34]. For example, if a cell's resistance is R_0 at 100% State of Health (SOH), it increases to $1.25R_0$ when capacity drops to 80% SOH. Although it may not represent the real relationship between capacity fade and resistance increase, this simplified method enables the model to approximate resistance changes as degradation progresses. It is noted that this simplified method may under-represent the resistance-driven power fade. Future work will be conducted to improve the model accuracy when the resistance data is available.

Second, the predicted capacity and resistance values are fed into an equivalent circuit model (ECM) to determine current distribution and terminal voltage within the battery module. This step explicitly accounts for the module's electrical topology, whether cells are arranged in series or parallel, and updates the cycling conditions for every simulation time step. The process iterates until the module reaches the defined end-of-life threshold.

Finally, a Monte Carlo framework is applied to perform multiple runs with varied initial conditions, capturing variability in cell performance and electro-thermal inconsistencies. The results are averaged to represent the module's overall behavior, thereby producing a more robust and realistic prediction of second-life battery aging. More details on module-level modeling can refer to [13].

Since the specific form factor and module design of the BESS are not available, the degradation model in this work is based on available cylindrical LFP cell data, focusing only on electrochemical aging effects. Mechanical degradation factors related to form factor, stack pressure, and module design should be incorporated once application-specific data from the deployed system becomes available. Additionally, the model assumes the proposed SLB systems will use the same cell form factor from the LFP experimental data, while noting that future designs may use different form factors (e.g., prismatic or pouch) with potentially different mechanical and thermal aging characteristics.

2.4. Economic Feasibility Analysis

The evaluation of the economic feasibility regarding the incorporation of SLBs in the Stanford EV bus charging station is based on the technoeconomic decision support model previously proposed. In this study, the original data-driven model in the model framework has been substituted with our newly developed semi-empirical model tailored specifically for LFP batteries. This updated model has been seamlessly integrated into the existing module-level degradation framework. This model framework comprises a module-level prediction model and an economic assessment model of SLBs. Initially, the prediction model is employed to simulate SLB degradation behaviors, enabling the calculation of the SLB lifespan. Subsequently, leveraging the economic model allows for the estimation of SLB value based on factors such as their remaining useful life and other pertinent considerations.

More specifically, the economic model from our previous work estimates the maximum selling price of SLBs in different applications by calculating the net present value (NPV) of their future cash flows. This price represents the highest amount a customer would be willing to pay. Because SLBs compete directly with new batteries in the market, the maximum selling price after repurposing is determined by equating the NPV of an SLB to that of a new battery. Once the NPV of a new battery and the repurposing cost are known, the maximum value of an SLB can be derived. Additional details on the calculation methodology are provided in [13].

Diverse economic factors have been taken into account to explore the variations in SLB values across different scenarios. Under the assumption of no costs associated with obtaining SLBs, a calculation of cost savings derived from utilizing SLBs instead of new batteries is performed.

As per information provided by the Stanford Transportation Department, the requisite BESS for EV bus charging stations is approximated at 750 kWh in energy capacity and 300 kW in power capacity. Hence, our analysis is structured around these specifications to estimate the value of SLBs within this battery size. This approach allows for an economic evaluation based on the potential cost savings accrued by utilizing retired LFP batteries instead of procuring new ones.

3. Results and Discussions

3.1. Prediction Results of the Cell-level Aging Model

In this section, the primary aim is to show the prediction results of the developed cell-level aging model using experimental data from [28]. A comparative analysis is conducted between the model predictions and the actual degradation provided in the battery datasheet, as delineated in Figure 2. These curves depict the correlation between capacity loss and the number of cycles, showcasing a gradual reduction in battery capacity as the number of cycles increases. Here, capacity loss is defined as the percentage of capacity reduction compared to its initial capacity.

Figure 2 presents the prediction performance of the model across varying C-rates and temperatures. Figure 2(a) and (b) demonstrates an excellent concurrence between the model predictions and experimental data across all three temperatures. It is obvious that higher temperatures would accelerate battery aging. However, under the 2C cycling condition, the difference in degradation between 15°C and 25°C becomes much less pronounced. This is likely because at higher C-rates the cycling-induced degradation dominates, leaving less time for temperature-driven calendar aging processes to manifest compared to the 1C case, where longer cycle durations allow temperature effects to play a more significant role. Still, temperature effects become increasingly significant over longer operating periods. As a result, effective thermal management is essential for ensuring the longevity and reliability of second-life batteries. Commercial stationary energy storage systems (e.g., Honeywell Ionic™, BYD Chess Plus) typically employ forced-air or liquid cooling and active temperature monitoring to preserve battery health and safety over multi-year operation. Future implementations of SLBs for the Stanford EV bus charging station would similarly benefit from active thermal regulation to minimize temperature-induced degradation and improve long-term system performance and reliability.

Similarly, Figure 2(b)–(d) exhibits commendable model accuracy across diverse discharge C-rates. However, at a higher C-rate of 3C, a divergence emerges between the model predictions and experimental data, notably after 3000 cycles. This discrepancy likely arises due to accelerated degradation experienced by the battery at higher C-rates, a phenomenon not fully captured by the original model. This could be caused by both electrochemical and mechanical factors, including accelerated SEI layer growth, electrolyte decomposition, and lithium plating, as well as mechanical stress-induced particle cracking that damages the SEI layer and promotes further side reactions. Such degradation pathways are more pronounced at elevated C-rates and can lead to nonlinear capacity fade trends. While these effects are outside the intended operational envelope for the target SLB application (less than 1C), acknowledging them provides useful context for potential model refinement in future high C-rate studies.

Despite this observed discrepancy, the model maintains satisfactory performance within temperature and C-rate ranges pertinent to most second-life applications. It yields a MAE of approximately 3% and an impressive R^2 value of 96%. This validation underscores the model's reliability within its intended operational parameters, signifying its potential utility. This validation, while highlighting

FIGURE 2 Prediction results of cell-level aging model for LFP battery in comparison with the experiment datasheet. The experiment data is obtained from [28] and denoted as exp, where prediction results are denoted as pred. (a, b) 15°C, 25°C, and 35°C for 1C and 2C discharge rate; (c, d) 25°C for 0.5C and 3C discharge rate. All the cells were cycled from 0% to 100% SOC.

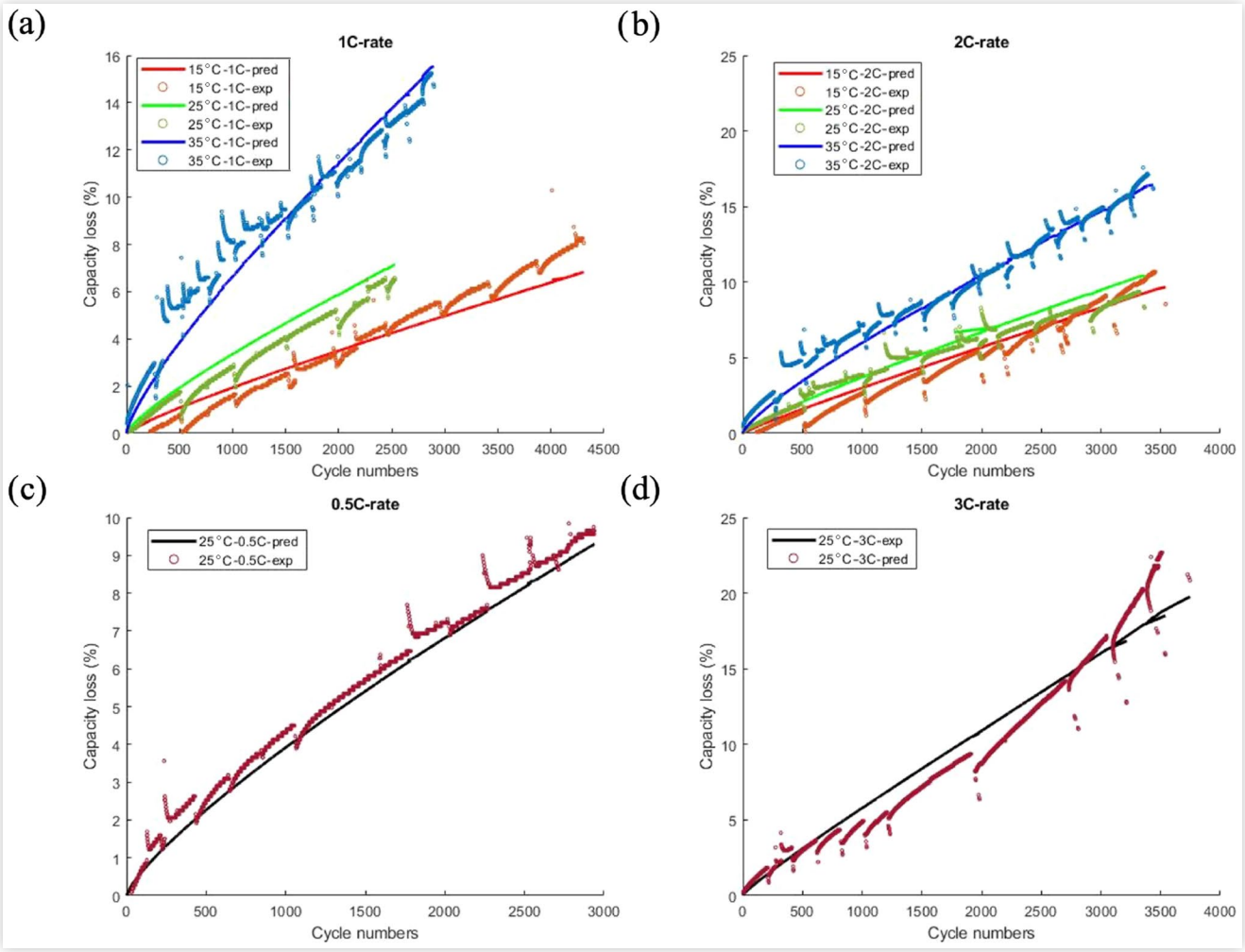

areas for enhancement, lays the groundwork for subsequent advancements in the model's predictive capabilities.

3.2. Simulation Results of Different Using Conditions

Equation 4 elucidates that battery degradation is mainly influenced by temperature and discharging C-rate. SOC is also another important factor, but due to a lack of experimental data, it is not discussed in this work. Here, we use Equivalent Full Cycle (EFC), which represents the cumulative amount of energy that has discharged from a battery, normalized to a full charge–discharge cycle at its nominal capacity, to compare battery degradation across different C-rates. Through an analysis of different temperature and discharging C-rate scenarios, we aim to discern their collective influence on battery degradation. Our objective is to identify the most favorable operational conditions that minimize degradation in SLBs utilized within EV bus charging stations. This investigation will aid in delineating an optimized usage protocol, enhancing the longevity and performance of the batteries in this specific application.

The analysis involved three distinct values for temperatures and four different C-rate values, as detailed in Table 3. Our baseline scenario stood at 25°C and 1C discharge current. Through simulation, the average battery degradation results were observed for each case, as depicted in Figure 3. It should be noted that from the Monte Carlo

TABLE 3 Different battery aging variables: C_{rate} represents the charging and discharging rate and T represents the battery operating temperature.

Variables	Values
C_{rate}	0.5C, 1C, 2C, 3C
T	15°C, 25°C, 35°C

FIGURE 3 The simulation results of LFP SLBs in different using conditions: (a) battery degradation under 15°C, 25°C, 35°C; (b) battery degradation under 0.5C, 1C, 2C, and 3C discharge current.

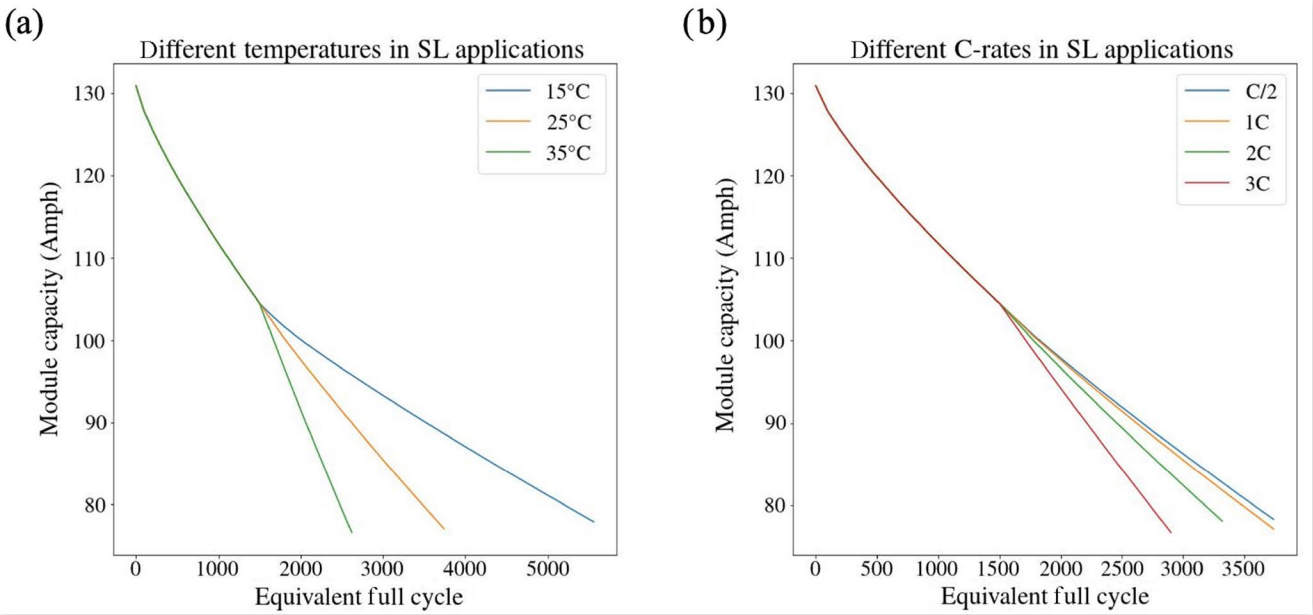

simulation, the resulting spread in predicted capacity was within 5%, demonstrating the uncertainty has a limited effect on the degradation predictions and does not change the key conclusions.

Figure 3(a) elucidates the impact of varied temperatures on battery degradation. Notably, lower temperatures, particularly from 35°C to 15°C, significantly extend battery life. However, it's important to consider that lower temperatures entail additional energy for cooling, thereby increasing operational costs. Therefore, maintaining the battery at 25°C appears more practical for this application. In Figure 3(b), the influence of the discharging C-rate is evident. Lower currents, specifically below 1C, exhibit minimal differences in battery lifetime. However, a significant reduction in total lifetime occurs at higher currents, particularly at 3C. Given that second-life applications typically don't demand such high currents, adhering to charging and discharging SLBs below 1C in EV bus charging stations appears viable.

Based on these findings, the recommended operating conditions for SLBs in EV bus charging stations would involve temperature control at 25°C and limiting discharge current to below 1C. These parameters aim to optimize battery longevity and performance while balancing operational costs and efficiency within this application scenario. The estimated lifetime of the battery in a second life is 6.3 years.

3.3. Sensitivity Analysis of Economic Model Variables

Based on the economic model, the valuation of SLBs is contingent upon several crucial factors. These pivotal determinants include the price of new batteries, revenue generated per unit in the second-life application, repurposing expenses, recycling value, initial SOH of retired batteries, and the extent of battery utilization in the second-life phase. Table 4 showcases the values of these influential factors, each subject to specific variations for the purpose of conducting a sensitivity analysis.

The baseline values for these factors have been derived from an extensive literature review and insights provided by the Stanford Transportation Department. However, in real-world scenarios, each of these factors is prone to variations.

Several assumptions are made on the selection of factor base values and variations: (1) Most factors were assumed to vary by ±20% across scenarios, with the exception of recycling value and battery SOH; (2) Recycling value can vary with technology maturity. For LFP batteries, reported values are often negative; therefore, in the base case, the recycling value is set to 0; (3) A negative recycling value represents a cost to recycle retired LFP batteries,

TABLE 4 Different economic factors with variations.

Variables	Base case	Variations
New battery price ($/kWh)	426 [35, 36]	341, 511
Initial SOH	80%	85%, 75%
Unit revenue ($/kWh)	0.55 [37]	0.44, 0.66
Recycling value ($/kWh)	0 [38]	–10, 10 [38]
Repurposing cost ($/kWh)	25 [38]	20, 30
Duty cycle per day	0.7	0.56, 0.84

The base case represents the SLB is used in the optimized working condition.

whereas a positive value reflects potential profit from future recycling technology. A variation range of ±10$/kWh is used, based on current estimates from the Chinese market [38], where LFP adoption is widespread and extensively studied; (4) Duty cycle values are based on estimates from the Stanford Transportation Department for a scenario involving five duty cycles per week; (5) The battery SOH in the base case is set to 80%. Since a ±20% variation is not realistic for this parameter, a smaller range of ±5% is adopted.

Our intention is to scrutinize the impact of these potential variations through a sensitivity analysis, offering insights into how alterations in each factor could affect the overall valuation of SLBs. This comprehensive analysis aims to provide a nuanced understanding of the economic viability and potential fluctuations that could impact the financial evaluation of SLBs. Figure 4 displays a sensitivity analysis of various factors influencing the pricing of SLBs. The investigation highlights that factors such as battery initial SOH, battery duty cycle in the second life, and new battery price exert substantial impacts on SLB selling prices. Generally, changes in these factors align with corresponding alterations in SLB prices. However, the unit revenue and duty cycle per day are two exceptions. Higher unit revenue increases the NPV of new batteries, making SLB price lower to maintain competitive pricing. Similarly, elevating the duty cycle per day accelerates the degradation rate of used batteries more than that of new batteries, resulting in reduced generated cash flows and subsequently lowering SLB prices.

The impact of initial SOH on pricing is particularly pronounced when SLBs operate at lower SOH levels. Lower SOH triggers accelerated degradation, significantly reducing the battery's second life, thus considerably impacting pricing. Conversely, recycling value and repurposing costs exert comparatively minor effects on SLB prices. However, they remain essential considerations, especially in anticipation of future technological developments, potentially leading to increased recycling values for LFP batteries.

3.4. Cost Reduction via Implementing Retired Batteries

As previously discussed in this section, assuming the acquisition of LFP batteries from Stanford's Marguerite bus fleet at no cost allows for the calculation of total cost savings incurred by utilizing these used batteries in their second life. Focusing solely on the base case scenario, the cost reduction amounts to $82,500 over 10 years, the entire second-life period, in comparison to the deployment of new batteries. However, considering the influence of various factors on SLB's value, this cost reduction fluctuates. In an optimistic scenario, leveraging SLBs could lead to savings of $150,000 over 13 years, while in a less favorable scenario, the savings diminish to $20,250 within a 5-year operational span. Additionally, even when assuming an SLB acquisition cost of $50/kWh, the system still yields a positive cost benefit. For example, with a 300 kWh SLB, the total cost reduction remains positive at approximately $5000, even under conservative (unfavorable) conditions. This comprehensive analysis underscores the economic viability of SLBs for Stanford's EV bus charging station.

4. Future Work

The future studies should aim to further improve the model by incorporating dynamic cycling experimental

FIGURE 4 The simulation results of LFP SLBs in different using conditions.

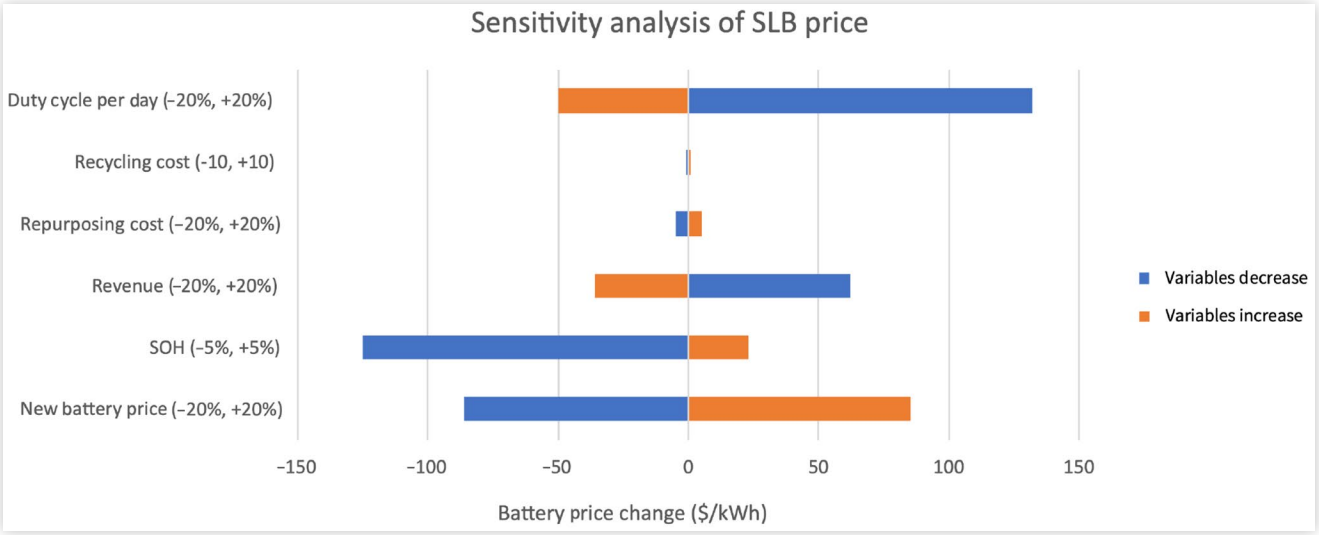

data for SLBs. The experiment data used in this study and most papers employed constant charging and discharging currents alongside fixed cut-off voltages. However, discrepancies persist between the experimental cycling conditions and real-life cases. Therefore, a more robust model can be developed by integrating these real-life duty profiles into the aging model. Moreover, future work should also focus on validating and refining the model once the actual SLB system design for the Stanford EV bus charging station is finalized. Once available, the module- and system-level parameters, such as module structure and cooling system design should be incorporated to include the mechanical effect on battery aging. More specifically, experimental cycling data from cells matching the deployed chemistry, form factor, electrode stacking method, and thermal management configuration should all be investigated and updated. This will enable more accurate representation of mechanical stress effects, swelling behavior, and heat dissipation characteristics.

Additionally, the current framework does not explicitly model rare safety-critical events such as lithium plating, internal shorts, or thermal runaway. While the intended second-life application operates under mild C-rates and controlled temperatures to mitigate these risks, future extensions could integrate physics-based models for such phenomena to enhance safety assessment. Furthermore, the long-term viability of SLBs in stationary applications depends on robust Battery Management System (BMS) functionality, including cell balancing, thermal monitoring, and fault detection. Without such measures, even minor voltage imbalances can trigger premature discharge cut-off, reducing available capacity and undermining economic performance. Future work should incorporate BMS operation and balancing strategies into the modeling framework to better capture system-level performance over long-term timescales.

From economic perspective, to enhance the model's accuracy, future research could integrate a dynamic recycling value, providing a more realistic estimation of SLB values. Additional research avenues could also delve into exploring a broader spectrum of applications, encompassing both on-grid and off-grid scenarios. Expanding the repertoire of potential use cases for SLBs would enrich the versatility of the technoeconomic decision support model.

5. Conclusion

This work has demonstrated the successful application of our developed technoeconomic decision support model in evaluating the economic viability of incorporating SLBs into Stanford University's EV bus charging station. It also shows the adaptability of the proposed framework to other battery chemistries, when the corresponding degradation models and parameters are available.

A semi-empirical aging model is developed for LFP batteries. Our simulations project that SLBs can endure for up to 10 years under optimized working conditions (<1C, 25°C, 20–80% SOC). Although the optimal operating range of the SOC cannot be provided in this work due to data limitations, this range is selected based on our previous work [13] and partial experiment data. The economic sensitivity analysis reveals that SLB's initial SOH, new battery price, and the duty cycle per day during the second-life application significantly impact the SLB's value. The potential cost reduction by employing SLBs instead of new battery ranges from $20,000 to $150,000 throughout the second life under various scenarios. These findings strongly advocate for SLB implementation as an energy storage system for Stanford University's EV bus charging station. Overall, this case study underscores the robustness of the technoeconomic decision support model in practical applications.

Conflict of Interest

The authors and SAE International declare that one of the authors of this article was on the editorial board of the journal. SAE warrants that confidentiality was maintained throughout the peer-review process and no partiality was granted to the work. SAE further warrants that the editorial board member had no influence and did not take part in any type of decision making or peer review.

Acknowledgements

This manuscript is based in part on the author's (Jihan Zhuang) doctoral dissertation "A decision-making model for retired Li-ion batteries," submitted to Stanford University in 2024. I confirm that I hold the rights to reuse all content from the dissertation, including figures and tables, and no transfer of copyright occurred.

This research is supported by the Stanford StorageX Initiative Circular Economy of Energy Storage (C2E2) consortium and Bits&Watts Initiative at Stanford University.

Declaration of AI-Assisted Technologies

The authors disclose that ChatGPT was used for correcting spelling and grammar mistakes. The authors have reviewed and edited all content as needed and take full responsibility for the scientific integrity and authenticity of this article.

Contact Information

Jihan Zhuang, first author, corresponding author
jihan123@stanford.edu

Sally Benson, principal corresponding author
smbenson@stanford.edu

References

1. Adami, C., "Stanford Transitions to 100 Percent Renewable Electricity as Second Solar Plant Goes Online," accessed March 24, 2022, https://news.stanford.edu/stories/2022/03/stanford-transitions-100-percent-renewable-electricity-second-solar-plant-goes-online.
2. Stanford Transportation, "Transportation Initiatives," accessed April 17, 2025, https://poshenergy.com/articles/energy-storage-systems-for-ev-fleet-charging-a-case-study-on-stanford-universitys-bus-depot#:~:text=However,%20Stanford%20purchased%20its%20first,and%20Stanford%27s%20electric%20bus%20fleet.
3. Moradipari, A., Tucker, N., Zhang, T., Cezar, G. et al., "Mobility-Aware Smart Charging of Electric Bus Fleets," in *2020 IEEE Power Energy Society General Meeting (PESGM)*, Montreal, QC, Canada, 2020, 1-5, doi:10.1109/PESGM41954.2020.9281897.
4. Bartolucci, L., Cordiner, S., Mulone, V., Santarelli, M. et al., "PV Assisted Electric Vehicle Charging Station Considering the Integration of Stationary First- or Second-Life Battery Storage," *Journal of Cleaner Production* 383 (2023): 135426, doi:https://doi.org/10.1016/j.jclepro.2022.135426.
5. Salek, F., Resalati, S., Morrey, D., Henshall, P. et al., "Technical Energy Assessment and Sizing of a Second Life Battery Energy Storage System for a Residential Building Equipped with EV Charging Station," *Appl. Sci.* 12, no. 21 (2022): 11103, doi:10.3390/app122111103.
6. Tong, S.J., Same, A., Kootstra, M.A., and Park, J.W., "Off-Grid Photovoltaic Vehicle Charge Using Second Life Lithium Batteries: An Experimental and Numerical Investigation," *Applied Energy* 104 (2013): 740-750, doi:https://doi.org/10.1016/j.apenergy.2012.11.046.
7. Hamidi, A., Weber, L., and Nasiri, A., "EV Charging Station Integrating Renewable Energy and Second-Life Battery," in *2013 International Conference on Renewable Energy Research and Applications (ICRERA)*, Madrid, Spain, 2013, 1217-1221, doi:10.1109/ICRERA.2013.6749937.
8. Martín, I.S., Braco, E., Martin, A., Sanchis, P. et al., "Integration of Second-Life Batteries in Residential Microgrids and Fast Charging Stations," in *2022 IEEE International Conference on Environment and Electrical Engineering and 2022 IEEE Industrial and Commercial Power Systems Europe (EEEIC/ICPS Europe)*, Prague, Czech Republic, 2022, 1-6, doi:10.1109/EEEIC/ICPSEurope54979.2022.9854414.
9. Berzi, L., Cultrera, V., Delogu, M., Dolfi, M. et al., "A Model for System Integration of Second Life Battery, Renewable Energy Generation and Mobile Network Station," in *2020 IEEE International Conference on Environment and Electrical Engineering and 2020 IEEE Industrial and Commercial Power Systems Europe (EEEIC/ICPS Europe)*, Madrid, Spain, 2020, 1-6, doi:10.1109/EEEIC/ICPSEurope49358.2020.9160747.
10. Kamath, D., Arsenault, R., Kim, H.C., and Anctil, A., "Economic and Environmental Feasibility of Second-Life Lithium-Ion Batteries as Fast-Charging Energy Storage," *Environmental Science & Technology* 54, no. 11 (2020): 6878-6887, doi:10.1021/acs.est.9b05883.
11. Rallo, H., Canals Casals, L., De La Torre, D., Reinhardt, R. et al., "Lithium-Ion Battery 2nd Life Used as a Stationary Energy Storage System: Ageing and Economic Analysis in Two Real Cases," *Journal of Cleaner Production* 272 (2020): 122584, doi:10.1016/j.jclepro.2020.122584.
12. Seger, P.V., Thivel, P.-X., and Riu, D., "A Second Life Li-Ion Battery Ageing Model with Uncertainties: From Cell to Pack Analysis," *Journal of Power Sources* 541 (2022): 231663, doi:10.1016/j.jpowsour.2022.231663.
13. Zhuang, J., Bach, A., van Vlijmen, B.H., Reichelstein, S.J. et al., "Technoeconomic Decision Support for Second-Life Batteries," *Applied Energy* 390 (2025): 125800.
14. Prada, E., Di Domenico, D., Creff, Y., Bernard, J. et al., "Simplified Electrochemical and Thermal Model of $LiFePO_4$-Graphite Li-Ion Batteries for Fast Charge Applications," *J. Electrochem. Soc.* 159, no. 9 (2012): A1508-A1519, doi:10.1149/2.064209jes.
15. Pinson, M.B. and Bazant, M.Z., "Theory of SEI Formation in Rechargeable Batteries: Capacity Fade, Accelerated Aging and Lifetime Prediction," *J. Electrochem. Soc.* 160, no. 2 (2013): A243-A250, doi:10.1149/2.044302jes.
16. Weaver, T., Allam, A., and Onori, S., "A Novel Lithium-Ion Battery Pack Modeling Framework - Series-Connected Case Study," in *2020 American Control Conference (ACC)*, Denver, CO, 2020, 365-372, doi:10.23919/ACC45564.2020.9147546.
17. Petit, M., Prada, E., and Sauvant-Moynot, V., "Development of an Empirical Aging Model for Li-Ion Batteries and Application to Assess the Impact of Vehicle-to-Grid Strategies on Battery Lifetime," *Applied Energy* 172 (2016): 398-407, doi:https://doi.org/10.1016/j.apenergy.2016.03.119.
18. Nájera, J., Arribas, J., de Castro, R., and Núñez, C., "Semi-Empirical Ageing Model for LFP and NMC Li-Ion Battery Chemistries," *Journal of Energy Storage* 72 (2023): 108016, doi:https://doi.org/10.1016/j.est.2023.108016.
19. Wang, J., Liu, P., Hicks-Garner, J., Sherman, E. et al., "Cycle-Life Model for Graphite-$LiFePO_4$ Cells," *Journal of Power Sources* 196, no. 8 (2011): 3942-3948, doi:https://doi.org/10.1016/j.jpowsour.2010.11.134.
20. Severson, K.A., Attia, P.M., Jin, N., Perkins, N. et al., "Data-Driven Prediction of Battery Cycle Life before Capacity Degradation," *Nature Energy* 4, no. 5 (2019): 383-391, doi:10.1038/s41560-019-0356-8.

21. Attia, P.M., Grover, A., Jin, N., Severson, K.A. et al., "Closed-Loop Optimization of Fast-Charging Protocols for Batteries with Machine Learning," *Nature* 578, no. 7795: 397-402, doi:10.1038/s41586-020-1994-5.
22. Vermeer, W., Chandra Mouli, G.R., and Bauer, P., "A Comprehensive Review on the Characteristics and Modeling of Lithium-Ion Battery Aging," *IEEE Transactions on Transportation Electrification* 8, no. 2 (2022): 2205-2232, doi:10.1109/TTE.2021.3138357.
23. Sarasketa-Zabala, E., Gandiaga, I., Rodriguez-Martinez, L., and Villarreal, I., "Calendar Ageing Analysis of a $LiFePO_4$/Graphite Cell with Dynamic Model Validations: Towards Realistic Lifetime Predictions," *Journal of Power Sources* 272 (2014): 45-57, doi:https://doi.org/10.1016/j.jpowsour.2014.08.051.
24. Monteiro, A., Filho, A.V.M.L., Dantas, N.K.L., Castro, J. et al., "Integrating Battery Energy Storage Systems for Sustainable EV Charging Infrastructure," *World Electric Vehicle Journal* 16, no. 3 (2025): 147, doi:10.3390/wevj16030147.
25. Honeywell, "Honeywell Ionic™ Modular," https://process.honeywell.com/us/en/products/energy-storage-solutions/battery-energy-storage-systems/honeywell-ionic-modular.
26. Maisch, M., "BYD Launches New C&I Highly Integrated Battery Storage Solution," *PV Magazine*, 2025, accessed April 7, 2025, https://www.pv-magazine.com/2025/04/07/byd-launches-new-ci-highly-integrated-battery-storage-solution/
27. Bach, A., Reichelstein, S., Onori, S., and Zhuang, J., "Fair Market Value of Used Capacity Assets: Forecasts for Repurposed Electric Vehicle Batteries," *The Accounting Review* 101, no. 2 (2025): 33-55, doi:https://doi.org/10.2308/TAR-2025-0024.
28. Preger, Y., Barkholtz, H.M., Fresquez, A., Campbell, D.L. et al., "Degradation of Commercial Lithium-Ion Cells as a Function of Chemistry and Cycling Conditions," *J. Electrochem. Soc.* 167, no. 12 (2020): 120532, doi:10.1149/1945-7111/abae37.
29. Battery Archive, "Homepage of Battery Archive," https://www.batteryarchive.org/cycle_list.html?time=0001.
30. Sui, X., Świerczyński, M., Teodorescu, R., and Stroe, D.-I., "The Degradation Behavior of $LiFePO_4$/C Batteries during Long-Term Calendar Aging," *Energies* 14, no. 6 (2021): 1732, doi:10.3390/en14061732.
31. Broussely, M., Biensan, P., Bonhomme, F., Blanchard, P. et al., "Main Aging Mechanisms in Li Ion Batteries," *Journal of Power Sources* 146, no. 1 (2005): 90-96, doi:https://doi.org/10.1016/j.jpowsour.2005.03.172, Selected Papers Presented at *the 12th International Meeting on Lithium Batteries*.
32. Gwayi, I., Ayeng'o, S.P., and Kimambo, C.Z.M., "A Review of Lithium-Ion Battery Empirical and Semi-Empirical Aging Models for Off-Grid Renewable Energy Systems Application," *Engineering Reports* 7, no. 5 (2025): e70169, doi:https://doi.org/10.1002/eng2.70169.
33. Luh, M. and Blank, T., "Comprehensive Battery Aging Dataset: Capacity and Impedance Fade Measurements of a Lithium-Ion NMC/C-SiO Cell," *Scientific Data* 11, no. 1 (2024): 1004, doi:10.1038/s41597-024-03831-x.
34. Luo, G., Zhang, Y., and Tang, A., "Capacity Degradation and Aging Mechanisms Evolution of Lithium-Ion Batteries under Different Operation Conditions," *Energies* 16, no. 10 (2023): 4232, doi:10.3390/en16104232.
35. Viswanathan, V., Mongird, K., Franks, R., Li, X. et al., "2022 Grid Energy Storage Technology Cost and Performance Assessment," US Department of Energy, Washington, DC, 2022.
36. Cole, W., Frazier, A.W., and Augustine, C., "Cost Projections for Utility-Scale Battery Storage: 2021 Update," NREL/TP-6A20-79236, Technical Report, National Renewable Energy Laboratory, Golden, CO, 2021.
37. Yang, L. and Ribberink, H., "Investigation of the Potential to Improve DC Fast Charging Station Economics by Integrating Photovoltaic Power Generation and/or Local Battery Energy Storage System," *Energy* 167 (2019): 246-259, doi:10.1016/j.energy.2018.10.147.
38. Lander, L., Cleaver, T., Rajaeifar, M.A., Nguyen-Tien, V. et al., "Financial Viability of Electric Vehicle Lithium-Ion Battery Recycling," *iScience* 24, no. 7 (2021): 102787, doi:https://doi.org/10.1016/j.isci.2021.102787.